



Epigenetic transgenerational inheritance of vinclozolin induced mouse adult onset disease and associated sperm epigenome biomarkers

Carlos Guerrero-Bosagna¹, Trevor R. Covert¹, Md. M. Haque, Matthew Settles, Eric E. Nilsson, Matthew D. Anway, Michael K. Skinner*

Center for Reproductive Biology, School of Biological Sciences, Washington State University, Pullman, WA 99164-4236, United States

ARTICLE INFO

Article history:

Received 4 January 2012
Received in revised form
19 September 2012
Accepted 24 September 2012
Available online 2 October 2012

Keywords:

Epigenetic
Transgenerational inheritance
Mouse
Endocrine disruptor
DNA methylation

ABSTRACT

The endocrine disruptor vinclozolin has previously been shown to promote epigenetic transgenerational inheritance of adult onset disease in the rat. The current study was designed to investigate the transgenerational actions of vinclozolin on the mouse. Transient exposure of the F0 generation gestating female during gonadal sex determination promoted transgenerational adult onset disease in F3 generation male and female mice, including spermatogenic cell defects, testicular abnormalities, prostate abnormalities, kidney abnormalities and polycystic ovarian disease. Pathology analysis demonstrated 75% of the vinclozolin lineage animals developed disease with 34% having two or more different disease states. Interestingly, the vinclozolin induced transgenerational disease was observed in the outbred CD-1 strain, but not the inbred 129 mouse strain. Analysis of the F3 generation sperm epigenome identified differential DNA methylation regions that can potentially be utilized as epigenetic biomarkers for transgenerational exposure and disease.

© 2012 Elsevier Inc. All rights reserved.

1. Introduction

Although the current paradigm for disease etiology primarily involves genetic or DNA sequence mutation mechanisms, the majority of disease states have not been linked to specific genetic abnormalities or DNA sequence change. In addition, the majority of environmental factors known to influence disease do not have the capacity to alter DNA sequence [1,2]. Therefore, additional molecular mechanisms need to be considered in disease etiology and how environmental factors can promote disease. A factor to consider in disease etiology is the importance of early life exposures and events that are critical in later adult onset disease [3]. These developmental origins of disease require a molecular mechanism that does not involve the induction of genetic abnormalities or alterations in DNA sequence. A molecular mechanism that has been shown to mediate the actions of environmental factors on disease is epigenetics [1,2,4]. Epigenetics is defined as molecular factors and processes around DNA that regulate genomic

activity independent of DNA sequence, and that are mitotically stable [1,5]. Epigenetic processes include DNA methylation, histone modifications, chromatin structure changes, and some non-coding RNAs [1,6–11]. The current study is focused on an investigation of how an environmental compound (endocrine disruptor) can promote the epigenetic transgenerational inheritance of adult onset disease states. DNA methylation is investigated since it is the primary epigenetic mechanism previously shown to mediate generational inheritance through the male germ line [1,12].

Endocrine disruptors are a class of chemical compounds readily available in the environment that are known to influence development and disease [1,2,13–15]. A number of studies have reported a correlation between endocrine disruptor actions and epigenetic changes [12,16–20]. Previous studies have used the endocrine disruptor vinclozolin as a model environmental compound to investigate epigenetic transgenerational inheritance of disease. Epigenetic changes [12,16] have been correlated with the incidence of transgenerational disease in rats after developmental exposure to the endocrine disruptor vinclozolin [1,2,12,16,21,22]. The process leading to epigenetic transgenerational changes involves a critical period during germ line epigenetic programming in which vinclozolin acts to permanently alter the germ-line (i.e. sperm) epigenome [1,12,16]. The subsequent generations (F1–F3) following the initial exposure develop a variety of transgenerational adult onset diseases in the rat [1,12,21,22]. These include spermatogenic defects, testis abnormalities, prostate disease, kidney disease, immune abnormalities and female reproductive defects

Abbreviations: MeDIP, methylated DNA immunoprecipitation; Chip, tiling microarray chip; PCR, polymerase chain reaction; DMSO, dimethyl sulfoxide; E7–E13, embryonic day 7–13; V1, 100 mg/kg-d vinclozolin dose; V2, 200 mg/kg-d vinclozolin dose.

* Corresponding author. Tel.: +1 509 335 1524; fax: +1 509 335 2176.

E-mail address: skinner@wsu.edu (M.K. Skinner).

¹ These authors contributed equally to this study.

[12,21,23–25]. The current study was designed to extend these previous epigenetic transgenerational inheritance observations in the rat model [1,12] using the mouse model. This study was not designed for risk assessment, but to determine the potential that vinclozolin promotes transgenerational adult onset disease in the mouse. In addition, advanced epigenetic technologies [16] are used to identify epigenetic sperm biomarkers of transgenerational exposure and disease.

In the current study, vinclozolin is used as a model endocrine disruptor with anti-androgenic activity. Vinclozolin ((RS)-3-(3,5-dichlorophenyl)-5-methyl-5-vinyl-1,3-oxazolidine-2,4-dione) is a systemic fungicide registered for use on fruits and vegetables and commonly used in the wine industry [26]. Rat embryonic exposure to vinclozolin promotes abnormal male sexual differentiation and development, as well as adult spermatogenesis [12,27,28]. Vinclozolin exposure of gestating female rats (F0 generation) prior to and during the period of gonadal sex determination, embryonic day 8–14 (E8–E14), has been shown to reduce the spermatogenic capacity of subsequent F1–F4 generation male rats [12,23], while exposure to vinclozolin later in gestation (e.g. E15–E20) had no effect on adult spermatogenesis [27,28]. Flutamide is an androgen receptor antagonist previously used as a model anti-androgenic therapy [29–31], and shown to promote reproductive defects in rodents if administered prenatally [32]. In comparing the actions of vinclozolin and flutamide it was found that flutamide promoted an F1 and F2 generation phenotype, but not a transgenerational F3 generation phenotype, similar to that induced by vinclozolin [29]. Since the F1 and F2 generations involve direct exposure, the F3 generation is the first generation not involving direct exposure [33,34]. The F3 generation is used in the current study to assess epigenetic transgenerational inheritance in the mouse.

The transgenerational actions of vinclozolin appear to involve an epigenetic (i.e. DNA methylation) reprogramming of the male germ line [12,16]. A recent independent study has demonstrated a transgenerational effect of vinclozolin on DNA methylation of several imprinted genes in a mouse model [35]. A study in an outbred strain of mice also showed that gestational exposure to parental oral vinclozolin produces a reduction in sperm count and sperm head abnormalities [36]. Other environmental factors shown to promote epigenetic transgenerational inheritance of disease or phenotypes include the plasticizers bisphenol A (BPA) [37,38] and phthalates [38], dioxin [38,39], pesticides [12,38], hydrocarbons [38] and nutrition [40–42]. Therefore, a number of environmental factors can promote epigenetic transgenerational inheritance of adult onset disease. Epigenetic transgenerational inheritance has been demonstrated in worms [43], flies [44], plants [45], and mammals [12,46–48], suggesting this phenomenon is critical in biology and disease etiology [1]. The current study was designed to investigate the potential epigenetic transgenerational actions of vinclozolin on adult onset disease in the mouse.

The critical period of exposure is fetal gonad sex determination [1,2,5] which involves testis determination that is initiated by the expression of the sex determining region of the Y chromosome (Sry) gene [49]. Gonadal sex determination and testis cord formation occurs between E12 and E15 in the rat, while testis determination is initiated in the mouse embryo during E11–E12. The transgenerational phenotype induced in the rat [12] occurred when vinclozolin was administered at E8–E14 of gestation. Therefore, the treatment period of pregnant female mice (F0 generation) for the current study was adjusted earlier to E7–E13. During migration of the primordial germ cell down the genital ridge the germ cell genome (DNA) becomes demethylated upon colonization of the embryonic gonad [1,2]. At the onset of gonadal sex determination the germ line then is re-methylated in a sex specific manner [50]. Therefore, the exposure of an environmental factor during this period has the ability to alter the germ line epigenome and if

permanently modified can promote a transgenerational phenotype [12,16]. Therefore, the basic molecular mechanism proposed for environmentally induced epigenetic transgenerational inheritance of adult onset disease involves: (1) environmental exposure during the gonadal sex determination period; (2) alteration in the epigenetic programming (DNA methylation) of the primordial germ cell; (3) permanent alteration in the male germ line epigenome with imprinted-like programming that escapes the de-methylation of DNA at fertilization and during early embryonic development; (4) transmission of the altered sperm epigenome (DNA methylation) to subsequent generations in an imprinted-like manner; (5) altered epigenome and transcriptome in all cell types and tissues that develop from the sperm having an altered epigenome; and (6) increased susceptibility to develop adult onset disease. Previously, an inbred line of rat was found to be less responsive than an outbred line [12], so an inbred and outbred strain of mouse was compared. The current study investigates the ability of the model endocrine disruptors vinclozolin and flutamide delivered to pregnant female inbred 129 mice and outbred CD-1 mice (i.e. F0 generation) prior to and during the period of sex determination (E7–E13) to promote transgenerational adult onset disease in subsequent generations (i.e. F1–F3). A genome wide promoter epigenome (DNA methylation) analysis of the F3 generation sperm was performed to identify differential methylation regions that can potentially be used as epigenetic biomarkers of exposure and adult onset disease.

2. Material and methods

The general experimental design involved the transient exposure of gestating 129 inbred and CD1 outbred mice (Charles River, Wilmington, MA) during the period of gonadal sex determination, embryonic day 7–13 (E7–E13). The potential that inbreeding depression may influence vinclozolin induced transgenerational phenotypes was investigated through comparing the two mouse strains. Daily intraperitoneal injection of vinclozolin or flutamide during the exposure period was used. The F1 generation offspring were bred to generate an F2 generation and then F2 generation bred to generate the F3 generation animals. No sibling or cousin breeding was used to avoid any inbreeding conflicts. Animals were sacrificed before postnatal day 90 (P60–P90) and after 1 yr (>1 yr) age (12–17 mo) for pathology analysis and sperm collection. The pathology of testis, prostate, kidney and ovary were assessed at 12–17 mo and sperm number and motility at P60–P90. The sperm DNA was isolated to assess differential DNA methylation between control and vinclozolin lineage F3 generation samples. A methylated DNA immunoprecipitation (MeDIP) was performed and followed by a mouse promoter tiling array (Chip) using a comparative hybridization protocol [16]. The MeDIP-Chip differential DNA methylation sites identified were confirmed with a quantitative PCR analysis.

2.1. Animal protocols and *in vivo* treatments

Timed pregnant inbred 129 mice were given intraperitoneal injections with vinclozolin (100 mg/kg-d, 99% pure; ChemService, West Chester, PA), flutamide (20 mg/kg-d, Sigma, St. Louis, MO) or vehicle dimethylsulfoxide (DMSO) in sesame oil (vehicle) (Sigma, St. Louis, MO) as controls, while timed pregnant outbred CD-1 mice were given intraperitoneal injections (IP) with vinclozolin doses: 100 mg/kg-d (V1) or 200 mg/kg-d (V2) or DMSO in sesame oil as controls [23]. Mice were given injections from embryonic day (E) E7–E13, with plug date equal to day 0. Controls were injected with vehicle (DMSO) dose and were matched with vinclozolin or flutamide treatment animals within the same mouse strain at the time of injection and were analyzed together throughout all three generations. The number of F0 generation gestating females required to allow F3 generation animals to be acquired without sibling or cousin breedings were selected. The number of treated gestating females used were: for mouse 129 strain with 100 mg/kg-d dose (3 controls and 4 vinclozolin treated); for mouse 129 strain with flutamide 20 mg/kg-d dose (3 controls and 3 flutamide treated); and for mouse CD-1 strain with 100 mg/kg-d dose (V1) (4 controls and 3 vinclozolin treated) and used for mouse CD-1 strain with 200 mg/kg-d (V2) (3 vinclozolin treated). F1 postnatal (P) P90 males and females from different litters of control, vinclozolin and flutamide treatment groups were bred to generate the F2 generation. F2 generation mice were bred to generate the F3 generation. Breedings were carefully monitored to eliminate any sibling or cousin breeding to remove potential phenotypes as a result of inbreeding. The age matched male and female pairs were randomly selected from different litters for breeding with no other bias than avoiding any inbreeding. A subset of male mice were collected and analyzed between P60 and P90 for all generations and treatment groups. The number of P60–P90 males collected for replicates for the mouse 129 strain vinclozolin treatment group (i.e. *n* value) were: for F1 (8 control, 11 vinclozolin); for F2 (11 control, 22 vinclozolin); and for F3 (11 control, 11 vinclozolin). The number of

P60–P90 males collected for replicates for the mouse 129 strain flutamide treatment group were: for F1 (8 control, 8 flutamide); for F2 (9 control, 8 flutamide); and for F3 (8 control, 8 flutamide). The number of P60–P90 males collected for replicates for the mouse CD-1 strain vinclozolin treatment group were: for F1 (8 control, 6 V1, 8 V2); and for F2 (10 control, 10 V1, 6 V2). The numbers of greater than 1 yr age animals used are shown in the figures and tables. All procedures were approved by the Washington State University Animal Care and Use Committee (IACUC approval # 02568-026).

2.2. Sperm motility and concentration analyses

The sperm motility was determined using caudal epididymal sperm. The epididymis was dissected free of connective tissue and a small cut made to the cauda. The tissue was placed in 2 ml F12 culture medium (Fisher Scientific, USA) containing 0.1% bovine serum albumin (BSA) (Sigma, St. Louis, MO) for 10 min at 37 °C. Fifty microliters were placed on a warm slide and gently cover-slipped. The specimen was immediately examined using phase contrast microscopy with 200× magnification. The sperm motility assays examined rapid progressive, slow progressive and non-progressive motility according to WHO category [51]. The ratio of motile sperm to the total number of sperm, including immotile sperm, was calculated. Approximately 50–100 sperm were counted per microscopic field. The procedure was repeated at least twice with a new specimen from the same epididymis. Epididymal sperm count was determined using the same epididymis according to a previously described method with some modifications [27,52]. Briefly, the epididymis that was placed in the 2 ml of culture medium was minced. The tissue pieces were stored at 4 °C for 48 h to immobilize the sperm. Three independent sperm samples were counted using a hemocytometer. The counts were averaged and used as a replicate in statistical analysis. The control and vinclozolin generation analysis and the control and flutamide generation analysis for an individual experiment were done at the same time. All analyses were done blinded, such that different individuals were used for collection and counting.

2.3. Histology

The testes, epididymis, prostate, ovary and kidney were fixed in Bouin's fixative (Sigma, St. Louis, MO) for 2 h, washed in 70% ethanol and embedded in paraffin using standard procedures. Sections from each testis, epididymis, prostate, ovary and kidney were stained with hematoxylin and eosin (Sigma, St. Louis, MO) using standard procedures [21] for morphological analyses.

2.4. Pathology

Animal identification and treatment group were blinded to the researchers during analysis. Three individuals independently assessed the tissue histology and a minimum of two were required to agree to confirm the disease status. Data were tabulated for each abnormality based on the percentage of tissue with pathological changes per total tissue per cross-section in two tissue cross-sections. Mice developing tumors were submitted as whole animals or excised formalin-fixed tissue for tumor identification. All tissue cross-sections were stained with hematoxylin and eosin for analyses. The testis cross-sections were determined to be abnormal if the number of tubules with atrophy, vacuoles or germ cell agenesis was greater than 20% of the total tubules present in the testis cross section [23]. Renal lesions were diagnosed by an increase in morphologically identified tubular damage [21]. The kidney was considered abnormal if more than 30% of the tissue contained tubular lesions. Kidney abnormal changes involved extreme dilation with protein-rich fluids, fluid-filled cystic tubules, and thickening of the Bowman's capsule surrounding the glomerulus [21]. Ventral prostate tissue was considered abnormal if more than 30% of the prostatic ducts were atrophic and contained reduced columnar secretory epithelial cells [24]. Body and tissue (i.e., prostate, kidney, spleen, and testis) weights were monitored in age-matched adults. The Washington Animal Disease Diagnostic Laboratory at WSU was used for advice and performed necropsy in the event of other infrequent disease conditions.

2.5. Testicular cell apoptosis

The Fluorescein In Situ Cell Death Detection Kit (Roche Applied Science, Indianapolis IN) was utilized to detect apoptosis of testicular cells as described earlier [27]. The kit measures fragmented DNA from apoptotic cells by catalytically incorporating fluorescein-12-dUTP at the 3' DNA end using the enzyme terminal deoxynucleotidyl transferase (TdT), which forms a polymeric tail using the principle of the TdT-mediated dUTP Nick-End Labeling (TUNEL) assay. All the fluorescent cells in each testis section were counted at 400× magnification. The average number of fluorescent cells/whole testis cross section from one animal was used as a single value for statistical analysis. No significant change in tubule numbers per cross section was detected between the treatment lineages, so data was normalized per section.

2.6. Identification of ovarian cysts

Abnormalities in adult females of the F1, F2 and F3 generations were not extensively evaluated. However, at the time of sacrifice and dissection it was noticed that some females had cystic structures on their ovaries. These were grossly visible fluid-filled structures larger than normal Graffian follicles. If an animal had one or more cystic structures on one or both ovaries, then that female was considered to have cystic ovaries. A sub-set of 17 ovaries (CD-1 F3 generation control and V2 lineage) were also evaluated histologically, and there was concordance of ovaries labeled as cystic at gross dissection with the histologic presence of very large cystic structures. Cysts were defined as fluid-filled structures larger than antral follicles having a lining of none or a single layer of granulosa cells and an increased thickness of the surrounding stromal/thecal layer compared to what is found in large antral follicles.

2.7. Sperm head purification, DNA isolation and MeDIP

Sperm heads were separated from tails and purified following the protocol described [53] (without protease inhibitors) from a total of six CD-1 F3 vinclozolin (100 mg/kg-d dose) generation mice and six CD-1 F3 control generation mice in the range of 13–15 months of age. Sperm heads were then further purified using a 70% sucrose gradient centrifugation, based on the method described [54]. Purified sperm heads were resuspended in 1 ml buffer 0.5 M Tris-HCl, pH 8, 0.5 M ethylene diamine tetra-acetic acid (EDTA), 10% sodium dodecyl sulfate (SDS) and treated with 100 µl proteinase K (20 mg/mL) and 100 µl dithiothreitol (DTT) (0.1 M) at 55 °C for 1 h. DNA was precipitated with 50% isopropanol, washed with 70% ethanol and resuspended. Individual sperm DNA was used as samples for further methylated DNA immunoprecipitation (MeDIP) [16]. Two pools of samples (3 animals each from different litters and randomly selected) were produced for each experimental treatment (control and vinclozolin), therefore each pool contained different DNA samples from three different animals from different litters ($n=6$). The MeDIP was performed as follows: 6 µg of genomic DNA was subjected to a series of three 20 pulse sonications at 20% amplitude and the appropriate fragment size (200–1000 bp) was verified through 2% agarose gels; the sonicated genomic DNA was resuspended in 350 µl Tris-EDTA buffer (TE) and denatured for 10 min at 95 °C and then immediately placed on ice for 5 min; 100 µl of 5× IP buffer (50 mM Na-phosphate pH 7, 700 mM NaCl, 0.25% Triton X-100) was added to the sonicated and denatured DNA. An overnight incubation of the DNA was performed with 5 µg of antibody anti-5-methylcytidine monoclonal (Diagenode S.A., Denville, NJ) at 4 °C on a rotating platform. Protein A/G beads (Santa Cruz Biotechnology, Santa Cruz, CA) were prewashed in PBS-BSA 0.1% and resuspended in 40 µl 1× IP buffer. Beads were then added to the DNA-antibody complex and incubated 2 hr at 4 °C on a rotating platform. Beads bound to DNA-antibody complex were washed 3 times with 1 ml 1× IP buffer; washes included incubation for 5 min at 4 °C on a rotating platform and then centrifugation at 6000 rpm for 2 min. Beads-DNA-antibody complex were then resuspended in 250 µl digestion buffer (50 mM Tris-HCl pH 8, 10 mM EDTA, 0.5% SDS) and 3.5 µl of proteinase K (20 mg/ml) was added to each sample and then incubated overnight at 55 °C on a rotating platform. DNA purification was performed first with phenol and then with chloroform:isoamyl alcohol. Two washes and precipitations were then performed with 70% ethanol, 1 M NaCl and glycogen. MeDIP-selected DNA was then resuspended in 30 µl TE buffer. MeDIP sperm DNA was pooled into each of the four above mentioned groups, adding equal amounts of methylation enriched sperm DNA from each individual sample to the pools. Therefore, a total of four pools of MeDIP sperm DNA (CIP1, CIP2, VIP1 and VIP2) were used for the Chip arrays, with each pool containing MeDIP DNA from 3 different randomly selected animals from different litters.

2.8. Tiling array MeDIP-Chip analysis

Nimblegen Mouse Promoter 3 × 720 K format microarray (Mouse Ref Seq promoter array) (Nimblegen/Roche, Madison, WI) was used, each subarray contains 709,520 probes. These probes are of variable length from 50mers to 75mers. Each transcription start site tiled 2960 bps upstream and 740 bps downstream. The median probe spacing is 100 bps, the gap between the probe varying according to the exact length of the probe. There are 20,404 promoter regions for the mouse array. A total of 1 microarray, 3 sub-arrays, were used, one each for VIP1 versus CIP1, VIP2 versus CIP2 and then the last one has a dye-swap of the first one CIP1 versus VIP1.

Affymetrix' GeneChip® Mouse Promoter 1.0R Array was used (Affymetrix, Palo Alto, CA), which contains 4.6 million probes tiled that interrogate nearly 28,000 mouse promoter regions. These probes are 25-mer and tiled at an average resolution of 35 bp with gaps of approximately 10 bp between probes. Each promoter region covers approximately 6 kb upstream through 2.5 kb downstream of 5' transcription start sites. A total of 6 arrays were used, one each for CIP1, CIP2, VIP1 and VIP2, one for CIP1 + CIP2 and another for their DNA inputs, InpCIP1 + InpCIP2.

2.9. Bioinformatic and statistic analyses of chip data

For each hybridization experiment, raw data from both the Cy3 and Cy5 channels were imported into R (R Development Core Team (2010), R: A language for statistical computing, R Foundation for Statistical Computing, Vienna, Austria. ISBN 3-900051-07-0, URL <http://www.R-project.org>), checked for quality and converted

to MA values ($M = Cy5 - Cy3$; $A = (Cy5 + Cy3)/2$). The following normalization procedure was conducted. Within each array, probes were separated into groups by GC content and each group was separately normalized, between Cy3 and Cy5 using the Loess normalization procedure. This allowed for GC groups to receive a normalization curve specific to that group. After each array was normalized within array, the arrays were then normalized across arrays using the A-quantile normalization procedure.

Following normalization each probe within each array was subjected to a smoothing procedure, whereby the probe's normalized M values were replaced with the median value of all probe normalized M values across all arrays within a 600bp window. If the number of probes present in the window was less than 3, no value was assigned to that probe. Each probe's A values were likewise smoothed using the same procedure. Following normalization and smoothing each probe's M value represents the median intensity difference between vinclozolin generation and control generation of a 600 bp window. Significance was assigned to probe differences between vinclozolin generation (VIP1 and VIP2) and control generation (CIP1 and CIP2) by calculating the median value of the intensity differences as compared to a normal distribution scaled to the experimental mean and standard deviation of the normalized M . A Z-score and p -value were computed for each probe from that distribution. Clustered Regions of interest were then determined by combining consecutive probes with significance p -values less than 10^{-7} . The statistically significant differential DNA methylated regions were identified and p -value associated with each region presented. Each region of interest was then annotated for gene and CpG content. This list was further reduced to those regions with an average intensity value exceeding 9.5 (log scale) and a CpG density > 1%.

2.10. Quantitative PCR methylation analyses and motif search

The MeDIP-Chip differential DNA methylation sites identified were further tested with a quantitative PCR analysis [55,56]. Real time qPCR quantification of each significant region obtained from the array was performed on MeDIP samples and the values were normalized to the DNA concentration of MeDIP samples measured by picogreen (Life Technologies, Grand Island, NY). These qPCR assays were optimized and performed by the Genomics Core Laboratory at the University of Arizona, Tucson, AZ, as previously described [38]. For the motif analysis Glam 2 was used for creating a motif from the DMR [57] and STAMP was used to compare the created motif to known transcription factor binding sites [58].

2.11. Statistical analysis

For the litter size, weights and sperm analysis, data were analyzed with Student t -test in GraphPad Prism (GraphPad Prism Software, Inc., San Diego, CA). All values are expressed as the mean \pm SEM (standard error of the mean) of the parameter measured, unless stated otherwise. Differences were considered significant at $p < 0.05$. Statistical analyses were only done between control and vinclozolin or flutamide generation animals within each generation. Specific comparisons, analyses, and results are presented in the different figure legends.

3. Results

3.1. Transgenerational pathology analysis

The experimental design involved exposing gestating female inbred 129 strain and outbred CD-1 strain mice to daily intraperitoneal (IP) injections of vehicle (DMSO) (control) or vinclozolin between embryonic day 7 and 13 of gestation. The inbred 129 strain mice received 100 mg/kg-d (V1) dose and the CD-1 strain mice received doses of 100 mg/kg-d (V1) or 200 mg/kg-d (V2). In addition, a comparison was used with flutamide IP injections at a 20 mg/kg-d dose. The F1 generation males and females from different litters were bred to generate the F2 generation animals and F2 generation males and females from different litters were bred to generate the F3 generation animals, see Section 2. No sibling or cousin breedings occurred to avoid any inbreeding artifacts. The F1, F2 and F3 generation animals from postnatal P60–P90 or after 1 yr (12–17 mo) of age were analyzed for testis, sperm and other pathologies as previously described [12,21,23] from multiple lineages. All groups and exposure lineages were found to be similar and not to be statistically different for age range and litter representation.

The transient embryonic exposure to vinclozolin or flutamide in the mouse had no consistent transgenerational effects ($p > 0.05$) on litter size or male/female sex ratio in all generations analyzed. In addition, no consistent transgenerational differences were

observed in body weight, testis weight index, or kidney weight index with either vinclozolin or flutamide exposure, Tables S1A and S1B. Although selected generational effects were found, there was no consistent major vinclozolin or flutamide toxicity observed.

The mean number of apoptotic germ cells within the testes of male mice was increased in all the generations and ages analyzed (F1, F2, and F3 for P60–P90, F1 and F2 for >1 yr) of the 129 inbred strain vinclozolin lineage animal groups, Fig. 1a. There were no differences in apoptotic germ cells in the testis observed in the 129 strain mice flutamide lineage animals at any age or generation analyzed, Fig. 1b. The outbred mouse CD-1 strain V1 vinclozolin lineage groups showed significant increases in testicular apoptotic germ cells in the F1 and F3 P60–P90 groups and F1, F2, and F3 >1 yr groups, Fig. 1c. Interestingly, the low vinclozolin V1 dose had a more consistent spermatogenic cell defect (i.e. apoptosis) than the higher V2 dose in the CD-1 strain, Fig. 1. Whether this is a low dose bimodal dose curve remains to be elucidated. Therefore, vinclozolin induced a transgenerational (F1–F3) apoptotic spermatogenic cell defect in both the inbred 129 strain and outbred CD-1 strain mice. Apoptosis is a more sensitive physiological parameter than others in regards to epigenetic transgenerational inheritance phenotypes [12,21].

Transient fetal exposure to vinclozolin and flutamide (through the F0 generation gestating female) caused a reduction in the mean percentage of motile epididymal sperm primarily in the adult F1 generation males, Figure S1a–c. A reduction in mean epididymal sperm concentration was also primarily observed in the F1 generation vinclozolin lineage samples, Figure S1e. These reductions in mean sperm concentration were not observed in subsequent 129 mouse strain F2 or F3 generations. Although CD-1 strain vinclozolin mice showed reductions in mean epididymal sperm concentration for V1 mice in the F2 P60–P90 group and V2 mice in the F3 P60–P90 group, Figure S1f, all other ages and generations analyzed showed no significant differences between control and treatment groups. Therefore, the transgenerational effects on sperm motility and number were not consistent with treatment or generation.

In the aged F3 generation CD-1 strain mice, there were increases observed in the proportion of vinclozolin lineage mice exhibiting abnormal disease-like characteristics in testis, prostate, and kidney tissues analyzed, Fig. 2a. The >1-yr-old F3 vinclozolin generation CD-1 mice exhibited increased abnormalities in testicular tubules when compared to age-matched controls (Fig. 2b and c). In addition, vinclozolin F3 aged mice exhibited regression of prostatic secretory epithelium when compared to age-matched controls (Fig. 2d and e). The F3 >1 yr old vinclozolin lineage mice also had an increased percentage of cysts and thickened Bowman's capsules in the kidney (Fig. 2f and g). The number of >1 yr old animals evaluated are shown in Fig. 2a. The compiled data for individual animals, showing increased apoptosis, sperm concentration and motility, and disease states are presented for all F3 generation animals in Table S2. A combination of all the disease-like states indicated 75% of the vinclozolin lineage F3 generation animals developed at least one disease and 34% had two or more disease states, which was significantly different from controls ($p < 0.05$). In contrast to the CD-1 outbred mouse strain, the inbred 129 strain mice had no observable differences between treatment groups in adult onset disease of the prostate, kidney, testis or ovaries (data not shown). The control tissue histology shown in Fig. 2 was similar between the CD-1 and 129 strain mice. Therefore, the outbred strain appears more sensitive to vinclozolin induced transgenerational adult onset disease than the inbred strain of mouse.

A thorough analysis of pathology in the females was not performed. However, one major abnormal phenotype was observed in the ovaries of vinclozolin F1–F3 generation animals. A significant increase in ovarian cysts was observed in all F1–F3 generations of V2 vinclozolin females ($p < 0.05$), Fig. 3a. A larger number of ovarian

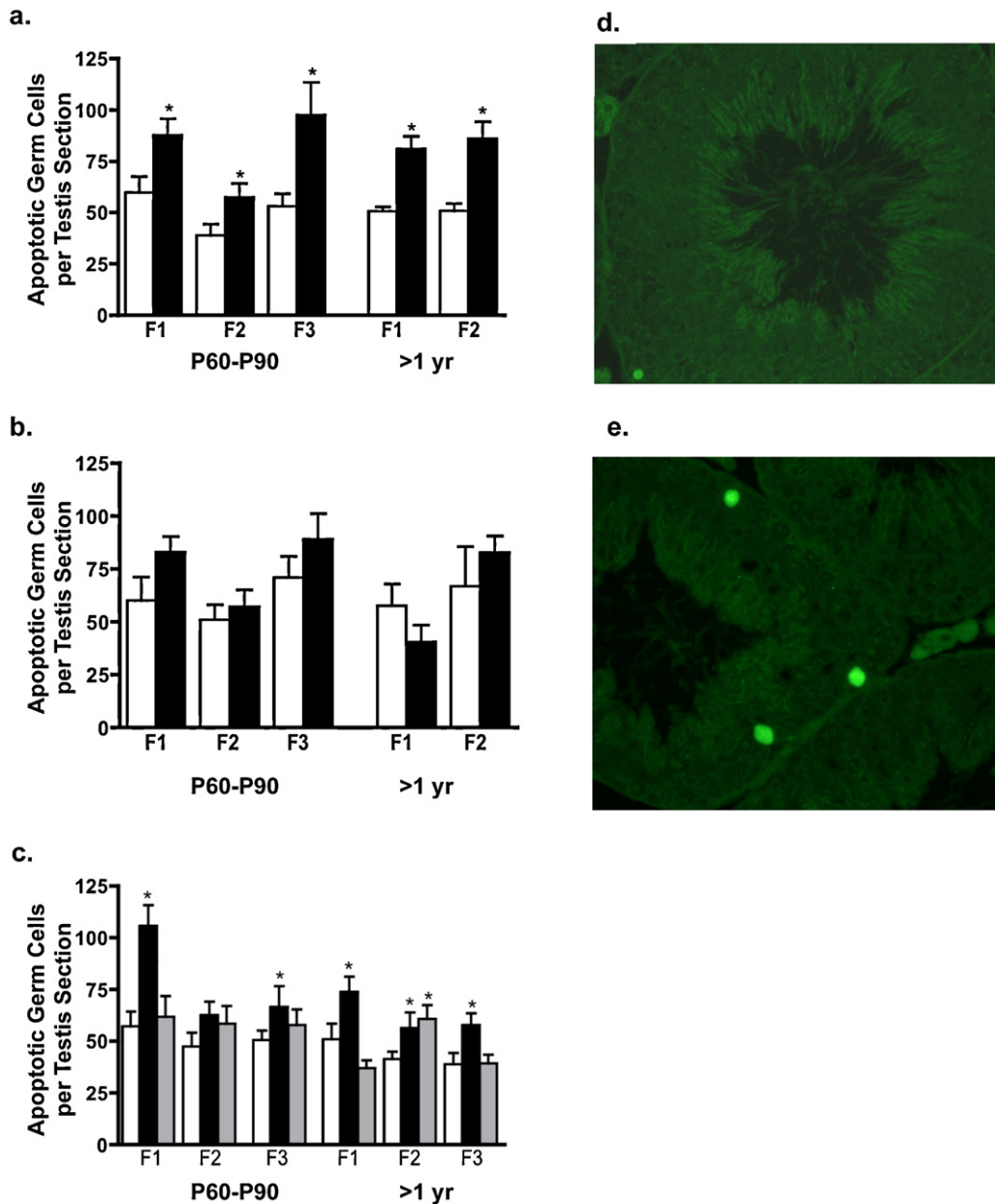


Fig. 1. Testicular spermatogenic cell apoptosis in (a) 129 mouse strain vinclozolin lineage, (b) 129 mouse strain flutamide lineage, and (c) CD-1 mouse strain vinclozolin lineage. The mean \pm SEM for control (white bars) and treated lineage (black bars). The CD-1 mouse vinclozolin lineage treatment of V1 (black bar) and V2 (gray bar) is presented. No significant difference in tubule cross section numbers was detected between treatment lineages or treatments. The asterisks (*) indicate a statistically significant difference ($p < 0.05$) between control and vinclozolin/flutamide lineage mice. The visible apoptotic cells (TUNEL assay) for control (d) and treated (e) testes are presented.

cysts were observed in the V2 and V1 dose vinclozolin lineage females. The ovarian cysts are shown in Fig. 3c and demonstrate a lack of granulosa cells and oocytes with a predominant theca cell layer present. Therefore, vinclozolin also induced a transgenerational female ovarian cyst phenotype.

3.2. Transgenerational effects on the sperm epigenome

The transgenerational F3 control and vinclozolin generation sperm epigenomes were analyzed with a methyl cytosine antibody for methylated DNA immunoprecipitation (MeDIP) followed by a genome wide promoter tiling array chip (MeDIP-Chip) assay [16]. The sperm DNA from F3 generation control and vinclozolin (100 mg/kg-d) lineage CD-1 outbred animals were analyzed. Two different experimental pools of control and vinclozolin lineage F3 generation MeDIP were generated ($n=6$), each containing

methylation enriched sperm DNA from 3 different animals from different litters. A comparative hybridization with the MeDIP-Chip assay was performed as described in Section 2 to identify differential DNA methylation between the control and vinclozolin sperm pools [16]. This analysis identified statistically significant differential DNA methylation regions (DMR) in 66 different promoters of average 800 bp in size, Table 1 and Table S3. The chromosomal locations of these differential methylation sites are presented in Fig. 4a as being increased or decreased in DNA methylation, Fig. 4b. Validation of MeDIP-Chip results was performed through real time quantitative PCR as previously reported [55,56]. Real time qPCR quantification of each significant region obtained from the array was performed on the MeDIP samples and the values were normalized to the DNA concentration in the MeDIP samples. Ratios of vinclozolin/control from the quantitative PCR (qPCR) analysis on the MeDIP sperm DNA pools were used to confirm the changes

Table 1
Regions showing vinclozolin-induced transgenerational change detected with MeDIP-Chip.

Gene symbol	Description	MGI ID	Entrez gene ID	Significance ($p \leq$)	Changed region coordinates			Region size (bp)
					Chr	Start	End	
Regions with MeDIP change in methylation confirmed by real time qPCR validation								
2310005E10Rik	Aldo-keto reductase family 1, member B10	1915111	67861	5.61E-10	6	34333365	34334132	767
5730403M16Rik	RIKEN cDNA 5730403M16 gene	1917764	108761	1.64E-08	7	7074813	7075523	710
Arl6ip4	ADP-ribosylation factor-like 6 interacting protein 4	1929500	65105	4.41E-08	5	124564910	124565615	705
Cdca5	Cdca5 cell division cycle associated 5	1915099	67849	2.65E-09	19	6082300	6082900	600
Ceacam-ps1	Carcinoembryonic antigen-related cell adhesion molecule pseudogene 1	3610557	100038912	4.18E-17	7	17243020	17244459	1439
Cwc22	CWC22 spliceosome-associated protein homolog to <i>S. cerevisiae</i>	2136773	80744	1.46E-16	2	77783335	77785070	1735
Dcxr	Dicarbonyl L-xylulose reductase	1915130	67880	1.16E-13	11	120588514	120591382	2868
Dhrs7	Dehydrogenase/reductase (SDR family) member 7	1913625	66375	1.42E-09	12	73768059	73768659	600
Egam-1c	Egam-1C	Predicted	100047130	2.00E-08	7	16486685	16487477	792
Elac1	ElaC homolog 1 to <i>E. coli</i>	1890495	114615	1.26E-08	18	73914746	73915346	600
Elf3	E74-like factor 3	1101781	13710	1.16E-18	1	137155288	137156184	896
Eml1	Echinoderm microtubule associated protein like 1	1915769	68519	2.30E-18	12	109646493	109647304	811
Etv1	Ets variant gene 1	99254	14009	2.75E-08	12	39504286	39505086	800
Gdf2	Growth differentiation factor 2	1321394	12165	9.77E-09	14	34751904	34752614	710
Guca1a	Guanylate cyclase activator 1a (retina)	102770	14913	9.73E-10	17	47537921	47538521	600
Hoxb2 (region2)	Homeobox B2	96183	103889	9.46E-08	11	96211360	96211960	600
Hsf1 or Bop1	Heat shock factor 1 or block of proliferation 1	96238 or 1334460	15499 or 12181	5.73E-08	15	76305346	76306056	710
Il22	Interleukin 22	1355307	50929	1.17E-08	10	117641731	117642331	600
Itgb3	Integrin beta 3	96612	16416	2.49E-10	11	104468315	104469310	995
Krt78	Keratin 78	1917529	332131	1.98E-08	15	101785650	101786540	890
Krtap1-4	1-4 keratin associated protein 1-4	3651229	629873	1.36E-13	11	99444032	99444716	684
Lif	Leukemia inhibitory factor	96787	16878	6.57E-10	11	4164487	4165167	680
Mro	Maestro	2152817	71263	1.52E-15	18	74017620	74018584	964
Ndufa8	NADH dehydrogenase (ubiquinone) 1 alpha subcomplex, 8	1915625	68375	8.10E-10	2	35903161	35903761	600
Nfe2l1	Nuclear factor, erythroid derived 2, -like 1	99421	18023	1.06E-09	11	96692937	96693537	600
Nkx6-3	NK6 homeobox 3	1921811	74561	2.09E-08	8	24262064	24262664	600
Olfir631	Olfactory receptor 631	3030465	258961	9.82E-08	7	111061151	111061751	600
Olfir978	Olfactory receptor 978	3030812	259109	4.47E-09	9	39801429	39802029	600
Pibf1 or Dis3	Progesterone immunomodulatory binding factor 1 or DIS3 mitotic control homolog (<i>S. cerevisiae</i>)	1261910 or 1919912	52023 or 72662	9.20E-09	14	99501070	99501670	600
Plekhh3	Pleckstrin homology domain containing, family G (with RhoGef domain) member 3	2388284	263406	5.19E-13	12	77632633	77633532	899

Table 1 (Continued)

Gene symbol	Description	MGI ID	Entrez gene ID	Significance ($p \leq$)	Changed region coordinates			Region size (bp)
					Chr	Start	End	
Pelo	Pelota homolog to Drosophila	2145154	105083	2.86E–15	13	115880977	115881882	905
Prelid1	PRELI domain containing 1	1913744	66494	2.06E–08	13	55425815	55426415	600
Reg1	Regenerating islet-derived 1	97895	19692	2.53E–09	6	78376091	78376691	600
Sepn1	Selenoprotein N, 1	2151208	74777	6.90E–09	4	134107080	134107680	600
Sepw1	Selenoprotein W, muscle 1	1100878	20364	6.75E–10	7	16509250	16510855	1605
Skap1	Src family associated phosphoprotein 1	1925723	78473	4.03E–22	11	96324250	96325444	1194
Slc35b1	Solute carrier family 35, member B1	1343133	110172	1.89E–12	11	95243522	95244222	700
Slmo2	Slowmo homolog 2 to Drosophila	1913640	66390	3.36E–09	2	174299251	174300078	827
St3gal2	ST3 beta-galactoside alpha-2,3-sialyltransferase 2	99427	20444	9.64E–09	8	113440826	113441426	600
Utp3	UTP3, small subunit (SSU) processome component, homolog to <i>S. cerevisiae</i>	1919230	65961	3.70E–11	5	88982036	88982731	695
Regions with MeDIP change in methylation not able to be tested with real time qPCR								
1700123K08Rik	RIKEN cDNA 1700123K08 gene	1923908	76658	3.87E–20	5	139004928	139005608	680
4930579J09Rik	RIKEN cDNA 4930579J09 gene	1915002	67752	1.38E–08	19	10559804	10560404	600
AK053193 (region1)	RIKEN cDNA E030030I06 gene	2442914	319887	1.23E–08	10	21869265	21869865	600
Alx3	Aristaless-like homeobox 3	1277097	11694	6.35E–08	3	107399690	107400290	600
gm6485	Predicted gene	3644007	624251	4.00E–10	3	104555956	104556734	778
Hoxb2 (region1)	Homeobox B2	96183	103889	3.27E–08	11	96209827	96210427	600
Iltf1b	Interleukin 10-related T cell-derived inducible factor beta	2151139	116849	2.54E–15	10	117732106	117732880	774
Lrrc61	Leucine rich repeat containing 61	2652848	243371	7.86E–23	6	48503482	48504082	600
Pcdha4	Protocadherin alpha 4	1298406	12936	1.85E–10	18	37113813	37114413	600
Rpl31	Ribosomal protein L31	2149632	114641	1.11E–12	1	39424522	39425122	600

The criteria for a qChip value to be considered as a change are:

- i) change is at least 1.2-fold increase or decrease regarding to control samples,
- ii) passed t -test with $p < 0.05$,
- iii) trend of the change observed in qChip is the same as observed in the Me-Dip Chip array.

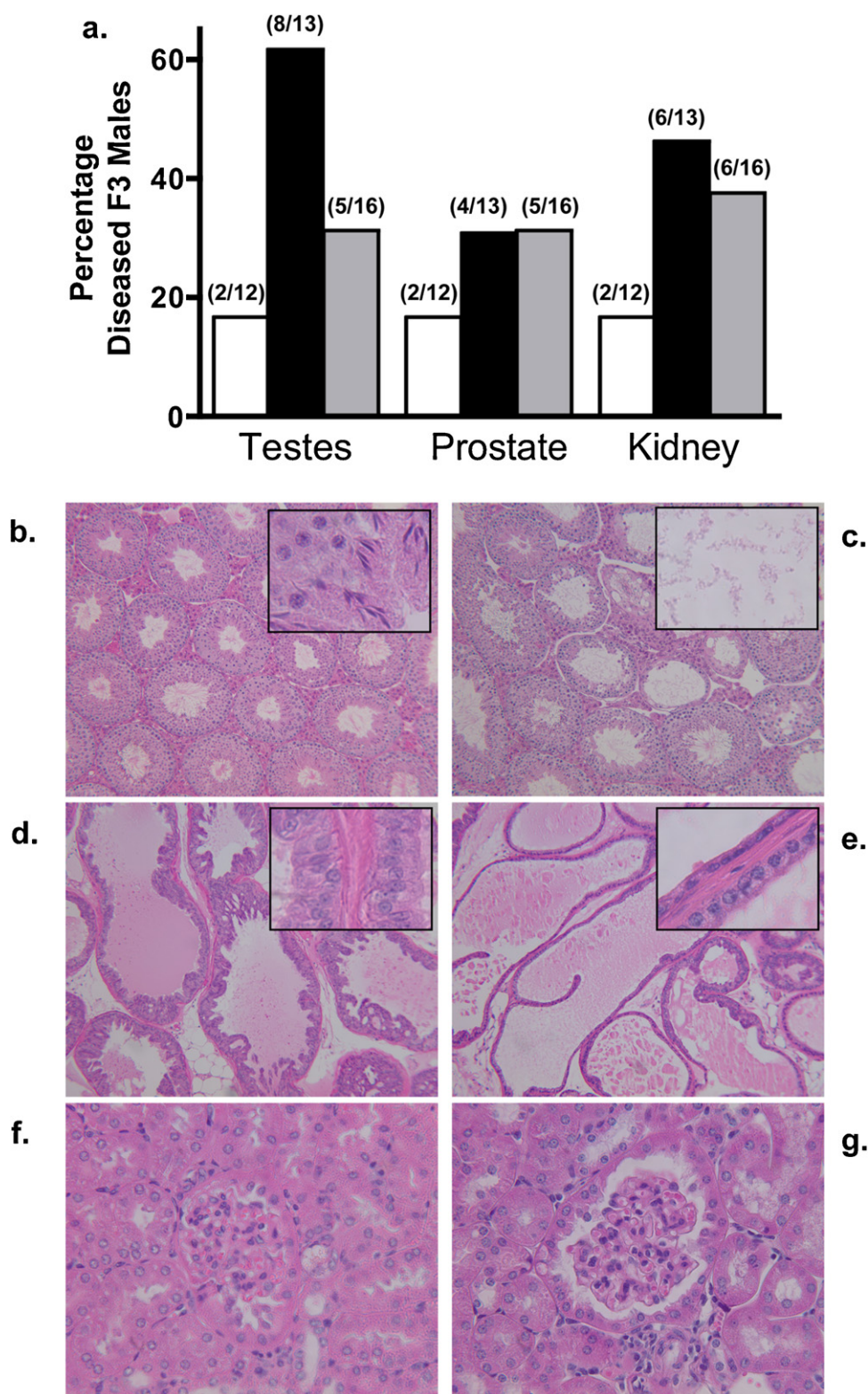


Fig. 2. Disease frequency presented as (a) percent of disease F3 generation males with the ratio of disease/total animal number presented above each bar for Control (white bar), V1 (black bar) and V2 (gray bar). Representative tissue micrographs from control (b, d, f) and V1 (c, e, g) F3 mice samples at >1 yr of age. (b) and (c) represent testis tubules cross sections at 100× magnification with 400× insets. (d) and (e) represent ventral prostate cross sections at 100× magnification with 400× insets. (f) and (g) represent kidney Bowman's capsule at 400× magnification.

observed in the tiling array and are presented in Fig. 4b. The combined tiling array data for each region that were confirmed or not able to be confirmed are shown in Fig. 4a and Figure S2. Some regions were not able to be confirmed due to technical limitations in the qPCR optimization. Approximately 25% of the sites were not

confirmed with qPCR of the MeDIP samples and are presented in Table S3. Two of these unconfirmed sites appeared to be hypervariable, indicating why they were not confirmed, but suggests they may be biologically important. The tiling array data for the sites with the largest increase (Elf3) and decrease (Mro) in methylation

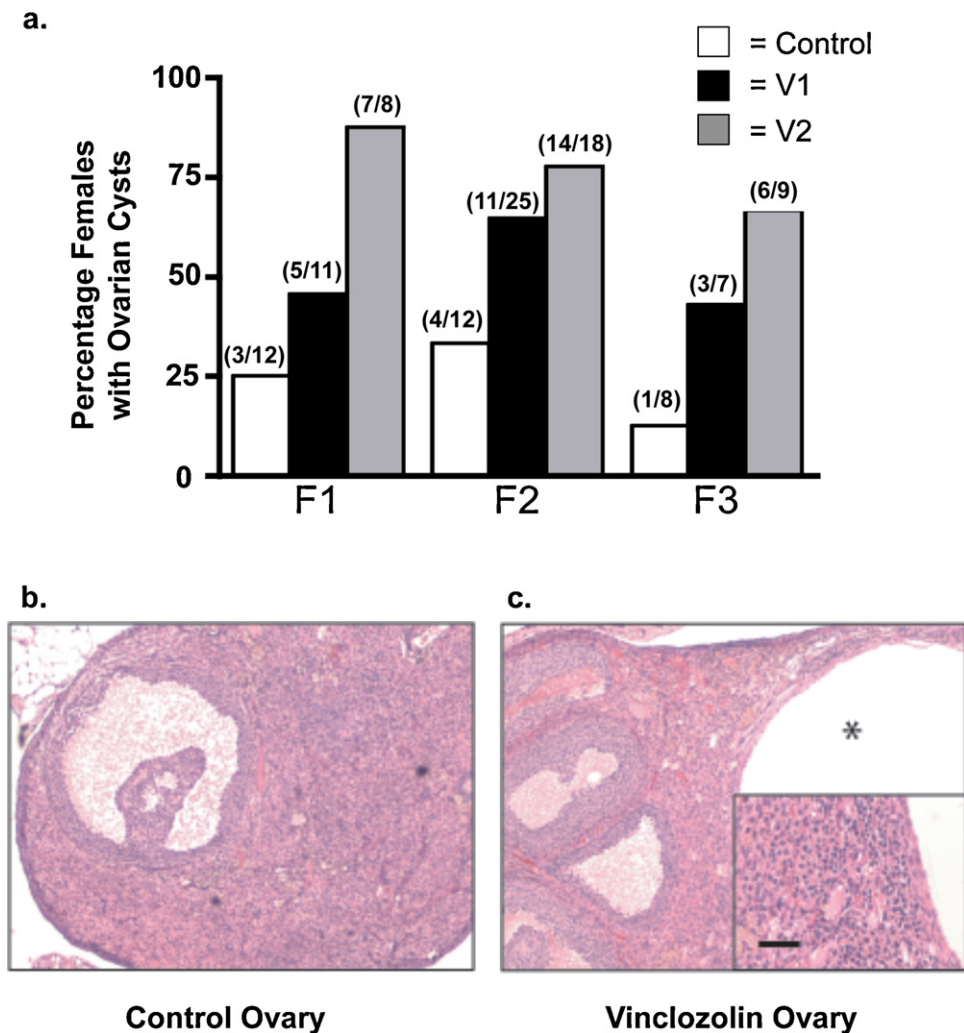


Fig. 3. (a) Percentage of ovarian cysts in aged vinclozolin female CD-1 mice. White bar represents control, black bar represents V1, gray bar represents V2. The ratio of animals with cystic ovaries/total animal number is presented above each bar. Representative histology of control (b) and vinclozolin (c) lineage ovaries are presented with asterisks indicating an ovarian cyst.

are shown in Fig. 5. Observations indicate 68 different DMR in 66 different promoters have transgenerational alterations in DNA methylation with the MeDIP-Chip analysis with 40 DMR confirmed with qPCR, Fig. 4. Previously 48 different promoters in rat sperm were identified with a comparative MeDIP-Chip analysis to have a transgenerational alteration in DNA methylation [16]. In a comparison of mouse and rat DMR, none of the gene promoters found in the mouse, Table 1, corresponded to the gene promoters identified in the rat sperm epigenome [16].

The MeDIP-Chip analysis presented in Table 1 and Fig. 4 involved the use of Nimblegen/Roche tiling arrays and a competitive hybridization of MeDIP samples (control versus vinclozolin) procedure [16]. An alternate procedure was used involving Affymetrix tiling arrays that require hybridization on two different chips and do not allow direct comparative hybridization. This procedure using duplicate arrays identified seven differential methylation regions, but none were confirmed (data not shown) using a bisulfite based PCR and mass spectrometry procedure [16]. Therefore, the MeDIP-Chip competitive hybridization approach used appears significantly more sensitive and accurate to identify differential methylation regions.

The previous analysis of transgenerational alterations in the rat sperm epigenome identified a consensus DNA sequence motif associated with a high percentage of promoter regions with

transgenerational change in DNA methylation in the rat sperm [16]. This (Environmental Induced Differential Methylation Consensus Sequence Motif 1) EDM1 was generated from the mouse sperm DMR in the current study and found to be similar to the EDM1 motif in the rat, Fig. 6a. The same known transcription factor binding sites were also present in the EDM1 mouse and rat motifs, Fig. 6b. Observations suggest a similar sequence motif (EDM1) genomic feature exists between species for the sperm DMR. An additional genomic feature investigated considered the CpG density of the differential DNA methylation regions (DMR). The majority of DMR identified had a 1–2% CpG density with a subsequent decrease as the density increased to >8%, Fig. 5c. Observations indicate the low density CpG density of 1–8% is more sensitive to transgenerational alterations than the high-density sites (e.g. CpG islands). The MeDIP-Chip analysis used is not biased for CpG content, while next generation sequencing is biased to high density CpG and currently cannot reliably analyze CpG densities <15–20 CpG/100 bp. Therefore, the MeDIP-Chip analysis was optimal for the current proposal.

4. Discussion

The current study was designed to investigate the transgenerational actions of vinclozolin on inbred and outbred strains of mice, and to identify epigenetic biomarkers in the sperm promoter

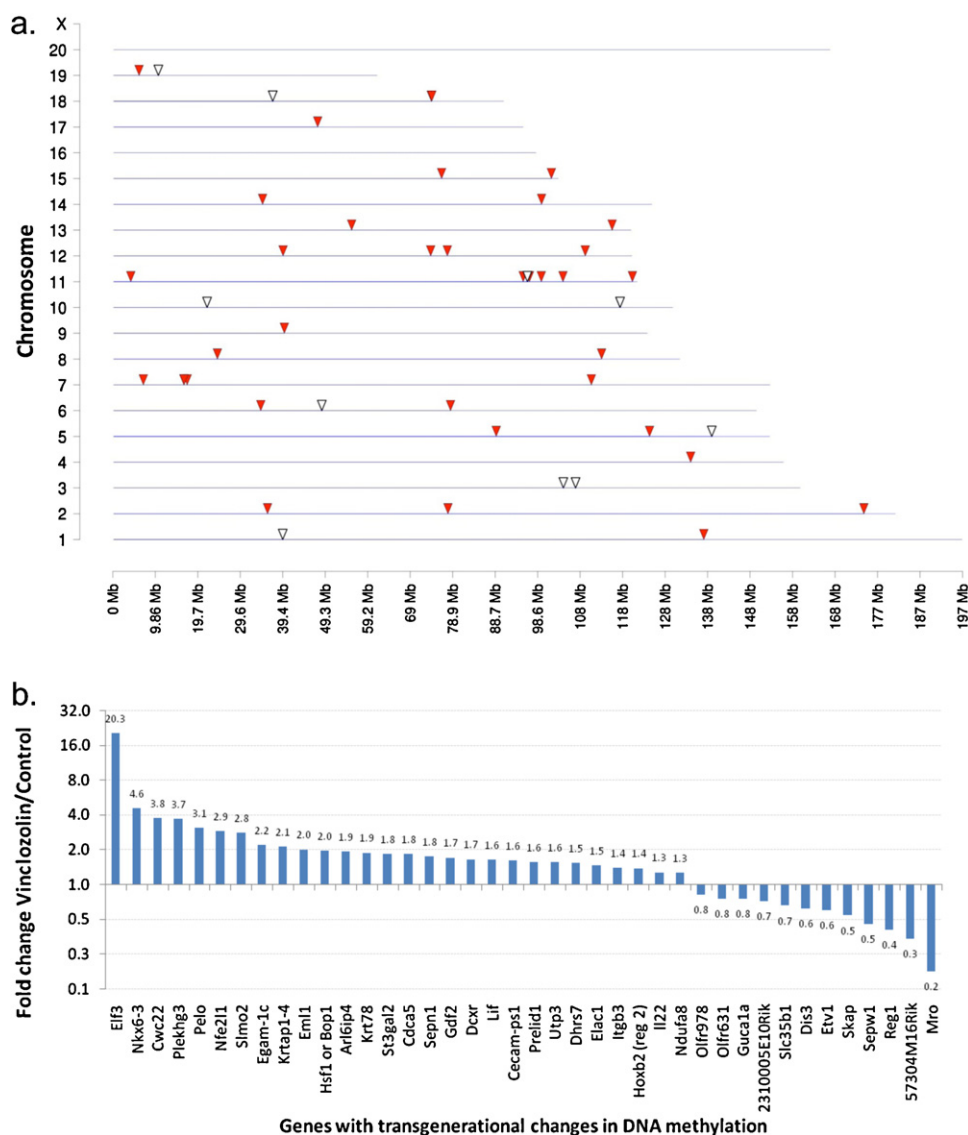


Fig. 4. Regions presenting vinclozolin-induced transgenerational change in F3 generation sperm DNA methylation: (a) chromosomal locations for regions detected with MeDIP-Chip to have transgenerational change in DNA methylation for regions confirmed (closed arrowhead) and not able to be tested (open arrowhead) with real time qPCR validation are shown; (b) real time qPCR validation of regions showing transgenerational change in methylation with values presented as fold change of Vinclozolin/Control and normalized by DNA concentration in the MeDIP samples. The criteria for a RT-qPCR value to be considered as a change are passed *t*-test with $p < 0.05$, and the trend of the change observed in the qPCR is the same as the observed in the MeDIP-Chip array.

epigenome. Gestating female mice during the developmental period of gonadal sex determination were transiently exposed to vinclozolin or flutamide to assess effects on transgenerational adult onset disease in the F1, F2 and F3 generations. The gestating females received daily intraperitoneal injections (IP) of pharmacologic doses of vinclozolin or flutamide. This study was designed to determine the potential to induce a transgenerational disease phenotype and investigate the molecular mechanisms involved, and was not designed to perform risk assessment or determine the potential environmental hazard of vinclozolin. Future toxicology studies are now needed for vinclozolin risk assessment using more appropriate modes of administration and environmentally relevant doses. The current study established the ability of vinclozolin to promote an epigenetic transgenerational inheritance of adult onset disease in the mouse model.

Analysis of litter size, sex ratio and body and tissue weights demonstrated no major toxicological effect of the vinclozolin or flutamide treatment on the F1 generation embryo exposed. Although some slight differences were observed with treatment

and generations, no consistent effect was observed. These observations are important to exclude major toxicity effects as the initial mechanism for the transgenerational phenotypes observed. Similar observations were found with the rat model for both vinclozolin [12,21,23,25] and flutamide [29].

The transgenerational actions of vinclozolin on spermatogenic cells were observed in both the inbred 129 mouse strain and the outbred CD-1 mouse strain. Previous observations have demonstrated that spermatogenic cell apoptosis is a more sensitive physiological parameter than others in regards to epigenetic transgenerational inheritance phenotypes [12,21]. The lower dose of vinclozolin had a more consistent action in the CD-1 mouse than the higher dose. The possibility this may reflect a low dose bimodal dose curve effect remains to be elucidated. The spermatogenic cell apoptosis was not observed after flutamide exposure for any generation examined. Previous studies have shown that flutamide can promote a spermatogenic cell defect in the F1 generation, but not the subsequent generations [29]. In this inbred 129 mouse strain flutamide had no effect on spermatogenic cell apoptosis. Therefore,

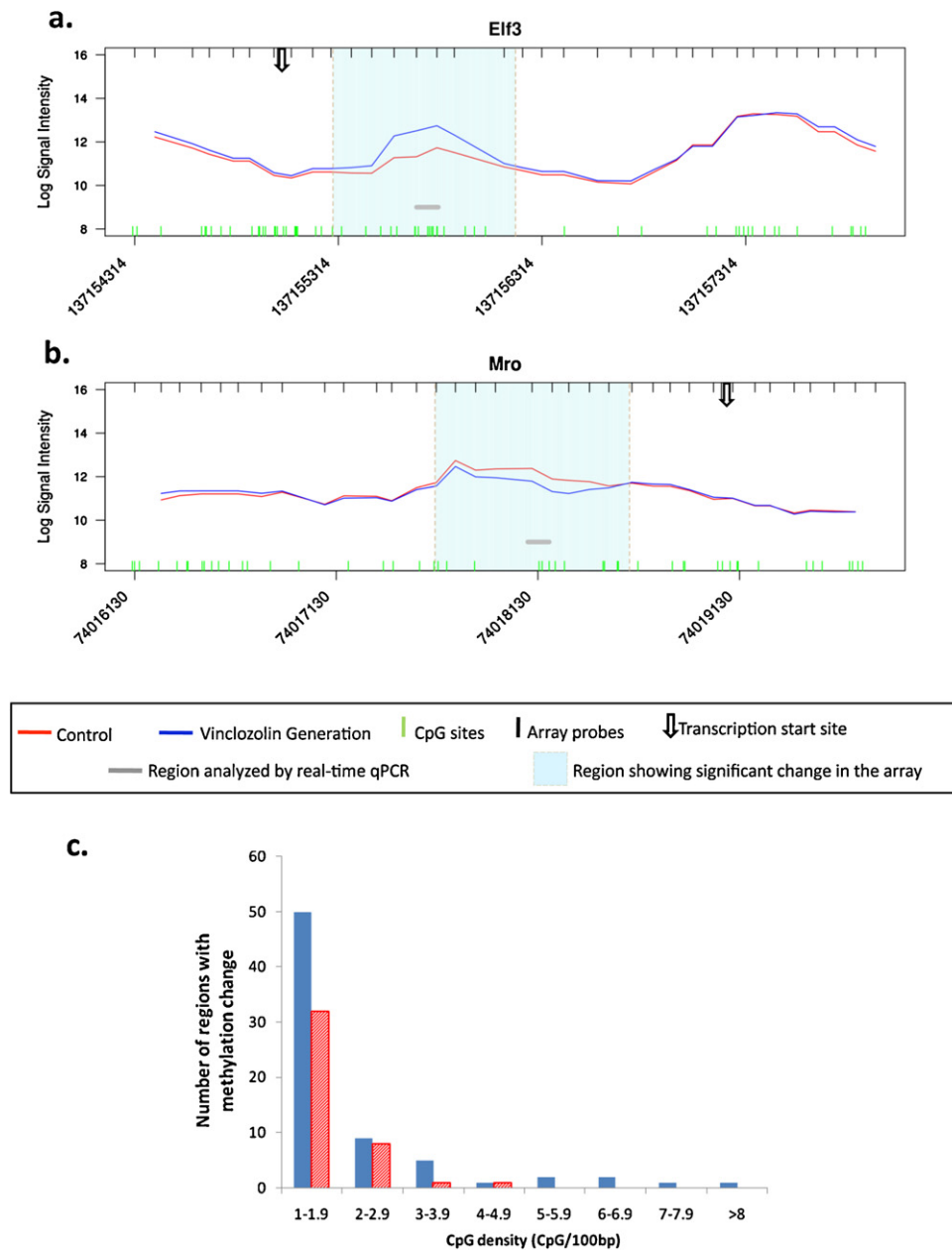


Fig. 5. Examples of tiling array data for the most dramatic changes in DNA methylation (a) *Elf3* or highest increase and (b) for *Mro*, for highest decrease. The log signal intensity for vinclozolin lineage, blue line, and control lineage, red line, is presented for chromosomal locations and the bar represents the site for qPCR confirmation. The distribution of differential methylation sites versus CpG density is shown in (c). Black bar represent all regions significantly changed in the MeDIP-Chip array and hatched bar shows only confirmed regions by real time qPCR. (For interpretation of the references to color in this figure legend, the reader is referred to the web version of this article.)

the actions of vinclozolin are not simply due to anti-androgenic actions, as previously suggested [29], but instead potentially due to alternate signaling events and/or metabolites. Current observations demonstrate that vinclozolin promotes a transgenerational spermatogenic cell defect in both an inbred and outbred strain of mouse. In contrast to previous observations in the rat, [12,23] no consistent effect was observed on sperm motility or numbers in the mouse, Figure S1.

Analysis of other adult onset disease-like conditions in the F3 generation male animals demonstrated abnormalities in the testis, prostate and kidney, Fig. 2. The testis abnormalities were associated with a loss of spermatogenic activity, reduction in germ cells per tubule cross section and increased number of tubules with no spermatogenic cells (azoospermia). The prostate disease-like abnormalities are associated with prostate epithelial cell atrophy,

periodic prostatitis and hyperplasia. The kidney disease-like abnormalities are associated with an increase in cysts and increase in the thickness of the Bowman's capsule. Previously, this kidney abnormality was shown to correlate with altered blood urea nitrogen (BUN) levels [12,21]. The increase in the frequency of abnormalities was similar for both doses of vinclozolin used. The induction of transgenerational onset disease by vinclozolin in this outbred CD-1 mouse, Fig. 2, is similar to the outbred Harlan Sprague Dawley rat previously described [12,21]. The incidence of disease was higher in the rat model, but similar in phenotype. Therefore, vinclozolin promoted a transgenerational inheritance of adult onset disease in the outbred mouse model.

In contrast to the outbred CD-1 mouse strain, the inbred 129 mouse strain had no detectable transgenerational phenotypes in the testis, prostate or kidney. Although a spermatogenic cell

of *Gcgr* and AK053193 genes. These hypervariable DMR may be important environmentally sensitive regulatory sites as previously suggested [2,66,67]. A mixture of 28 increased and 12 decreased DNA methylation sites were observed, Fig. 4. Interestingly, when a mouse sequence motif was generated from the mouse DMR a similar differential methylation motif 1 (EDM1) site as that found in rat sperm DMR was identified, Fig. 6. The similar EDM1 motif in mouse and rat sperm DMR suggests this genomic feature may be critical in the transgenerational programming of these sites. However, none of the mouse differential methylation sites had any overlap with the rat differential methylation sites previously identified [16]. Past comparison of imprinted genes between species has demonstrated distinct species specific sites suggesting the epigenomes of different species will for the most part be distinct [68]. The epigenetic transgenerational sperm epigenome sites identified in the mouse and rat are distinct. Although some genomic features may be similar, such as EDM1 and lower density CpG region sensitivity, the actual sites for the sperm differential DNA methylation regions are not similar. The mouse differential methylation promoters identified vary from transcription regulators (*Alx3*, *Hoxb3*) to cytoskeleton and extracellular matrix proteins (*keratin 8*, *integrin beta 3*), Table 1. The current study identified potential epigenetic biomarkers in the mouse sperm epigenome that identified animals that had an ancestral exposure to vinclozolin. In addition, these differential DNA methylation sites may act as biomarkers for the adult onset disease identified. The epigenetic transgenerational biomarkers are anticipated to be useful to potentially identify environmental exposures and provide early stage biomarkers for adult onset disease. This confirms a previous study with a number of different environmental toxicants promoting exposure specific epigenome biomarkers [38]. This study confirms the ability of vinclozolin to promote an epigenetic transgenerational inheritance of adult onset disease in the mouse model. The identification of the alterations of DNA methylation in the F3 generation sperm suggests a role of epigenetic modifications in the germ line as mediating the transgenerational phenotype. The objectives of the current study were to replicate the vinclozolin induced epigenetic transgenerational inheritance of adult onset disease in a mouse model and document sperm epigenome alterations. Although beyond the scope of the current study, future studies are now needed to investigate the epigenetic changes in the inbred 129 line, compare F1, F2 and F3 generation sperm epigenetic alterations, examine the somatic cell alterations, and clarify any biological connections with the potential epigenetic biomarkers identified. This epigenetic transgenerational inheritance is an important alternate mechanism to investigate in disease etiology from the current paradigm of the primarily genetic elements of disease etiology. The assumption is that a cooperative process of both epigenetics and genetics will be important for most disease. The ability of environmental factors to alter epigenetics provides a unique mechanism for environment to influence disease, independent of genetic abnormalities.

Acknowledgements

This manuscript is dedicated to the memory of Dr. Matthew D. Anway who passed away in April 2012. Matt played a significant role in the initial observations regarding vinclozolin induced epigenetic transgenerational inheritance of disease, as supported by his participation in the current study. We acknowledge the technical assistance of Ms. Sean Leonard, Ms. Keena Mullen and Mr. Shane Rekow, and thank Ms. Heather Johnson for assisting in preparation of the manuscript. This research was supported by a grant from the NIH, NIEHS to MKS.

Appendix A. Supplementary data

Supplementary data associated with this article can be found, in the online version, at <http://dx.doi.org/10.1016/j.reprotox.2012.09.005>.

References

- Skinner MK, Manikkam M, Guerrero-Bosagna C. Epigenetic transgenerational actions of environmental factors in disease etiology. *Trends in Endocrinology and Metabolism* 2010;21:214–22.
- Jirtle RL, Skinner MK. Environmental epigenomics and disease susceptibility. *Nature Reviews Genetics* 2007;8:253–62.
- Hanson MA, Gluckman PD. Developmental origins of health and disease: new insights. *Basic & Clinical Pharmacology & Toxicology* 2008;102:90–3.
- Skinner MK. Role of epigenetics in developmental biology and transgenerational inheritance. *Birth Defects Research Part C, Embryo Today: Reviews* 2011;93:51–5.
- Skinner MK. Environmental epigenetic transgenerational inheritance and somatic epigenetic mitotic stability. *Epigenetics* 2011;6:838–42.
- Chen ZX, Riggs AD. Maintenance and regulation of DNA methylation patterns in mammals. *Biochemistry and Cell Biology-Biochimie et Biologie Cellulaire* 2005;83:438–48.
- Craig JM. Heterochromatin—many flavours, common themes. *Bioessays* 2005;27:17–28.
- Fuks F. DNA methylation and histone modifications: teaming up to silence genes. *Current Opinion in Genetics and Development* 2005;15:490–5.
- Kim VN. Small RNAs just got bigger: Piwi-interacting RNAs (piRNAs) in mammalian testes. *Genes and Development* 2006;20:1993–7.
- Margueron R, Trojer P, Reinberg D. The key to development: interpreting the histone code? *Current Opinion in Genetics and Development* 2005;15:163–76.
- Wallace JA, Orr-Weaver TL. Replication of heterochromatin: insights into mechanisms of epigenetic inheritance. *Chromosoma* 2005;114:389–402.
- Anway MD, Cupp AS, Uzumcu M, Skinner MK. Epigenetic transgenerational actions of endocrine disruptors and male fertility. *Science* 2005;308:1466–9.
- Markey CM, Coombs MA, Sonnenschein C, Soto AM. Mammalian development in a changing environment: exposure to endocrine disruptors reveals the developmental plasticity of steroid-hormone target organs. *Evolution and Development* 2003;5:67–75.
- McLachlan JA. Environmental signaling: what embryos and evolution teach us about endocrine disrupting chemicals. *Endocrine Reviews* 2001;22:319–41.
- Edwards TM, Myers JP. Environmental exposures and gene regulation in disease etiology. *Environmental Health Perspectives* 2007;115:1264–70.
- Guerrero-Bosagna C, Settles M, Luckert BJ, Skinner MK. Epigenetic transgenerational actions of vinclozolin on promoter regions of the sperm epigenome. *PLoS ONE* 2010;5:e13100.
- Dolinoy DC, Huang D, Jirtle RL. Maternal nutrient supplementation counteracts bisphenol A-induced DNA hypomethylation in early development. *Proceedings of the National Academy of Sciences of the United States of America* 2007;104:13056–61.
- Guerrero-Bosagna CM, Sabat P, Valdovinos FS, Valladares LE, Clark SJ. Epigenetic and phenotypic changes result from a continuous pre and post natal dietary exposure to phytoestrogens in an experimental population of mice. *BMC Physiology* 2008;8:17.
- Tang WY, Newbold R, Mardilovich K, Jefferson W, Cheng RY, Medvedovic M, et al. Persistent hypomethylation in the promoter of nucleosomal binding protein 1 (*Nsbp1*) correlates with overexpression of *Nsbp1* in mouse uteri neonatally exposed to diethylstilbestrol or genistein. *Endocrinology* 2008;149:5922–31.
- Yaoi T, Itoh K, Nakamura K, Ogi H, Fujiwara Y, Fushiki S. Genome-wide analysis of epigenomic alterations in fetal mouse forebrain after exposure to low doses of bisphenol A. *Biochemical and Biophysical Research Communications* 2008;376:563–7.
- Anway MD, Leathers C, Skinner MK. Endocrine disruptor vinclozolin induced epigenetic transgenerational adult-onset disease. *Endocrinology* 2006;147:5515–23.
- Nilsson E, Larsen G, Manikkam M, Guerrero-Bosagna C, Savenkova M, Skinner M. Environmentally induced epigenetic transgenerational inheritance of ovarian disease. *PLoS ONE* 2012;7:e36129.
- Anway MD, Memon MA, Uzumcu M, Skinner MK. Transgenerational effect of the endocrine disruptor vinclozolin on male spermatogenesis. *Journal of Andrology* 2006;27:868–79.
- Anway MD, Skinner MK. Transgenerational effects of the endocrine disruptor vinclozolin on the prostate transcriptome and adult onset disease. *Prostate* 2008;68:517–29.
- Nilsson EE, Anway MD, Stanfield J, Skinner MK. Transgenerational epigenetic effects of the endocrine disruptor vinclozolin on pregnancies and female adult onset disease. *Reproduction* 2008;135:713–21.
- Kelce WR, Monosson E, Gamcsik MP, Laws SC, Gray LEJ. Environmental hormone disruptors: evidence that vinclozolin developmental toxicity is mediated by antiandrogenic metabolites. *Toxicology and Applied Pharmacology* 1994;126:276–85.

- [27] Uzumcu M, Suzuki H, Skinner MK. Effect of the anti-androgenic endocrine disruptor vinclozolin on embryonic testis cord formation and postnatal testis development and function. *Reproductive Toxicology* 2004;18:765–74.
- [28] Wolf CJ, LeBlanc GA, Ostby JS, Gray Jr LE. Characterization of the period of sensitivity of fetal male sexual development to vinclozolin. *Toxicological Sciences* 2000;55:152–61.
- [29] Anway MD, Rekow SS, Skinner MK. Comparative anti-androgenic actions of vinclozolin and flutamide on transgenerational adult onset disease and spermatogenesis. *Reproductive Toxicology* 2008;26:100–6.
- [30] Kassim NM, McDonald SW, Reid O, Bennett NK, Gilmore DP, Payne AP. The effects of pre- and postnatal exposure to the nonsteroidal antiandrogen flutamide on testis descent and morphology in the Albino Swiss rat. *Journal of Anatomy* 1997;190(Pt 4):577–88.
- [31] Okur H, Muhtaroglu S, Bozkurt A, Kontas O, Kucukaydin N, Kucukaydin M. Effects of prenatal flutamide on testicular development, androgen production and fertility in rats. *Urologia Internationalis* 2006;76:130–3.
- [32] Silversides DW, Price CA, Cooke GM. Effects of short-term exposure to hydroxyflutamide in utero on the development of the reproductive tract in male mice. *Canadian Journal of Physiology and Pharmacology* 1995;73:1582–8.
- [33] Skinner MK. What is an epigenetic transgenerational phenotype? F3 or F2. *Reproductive Toxicology* 2008;25:2–6.
- [34] Skinner MK. Metabolic disorders: fathers' nutritional legacy. *Nature* 2010;467:922–3.
- [35] Stouder C, Paoloni-Giacobino A. Transgenerational effects of the endocrine disruptor vinclozolin on the methylation pattern of imprinted genes in the mouse sperm. *Reproduction* 2010;139:373–9.
- [36] Elzeinova F, Novakova V, Buckiova D, Kubatova A, Peknicova J. Effect of low dose of vinclozolin on reproductive tract development and sperm parameters in CD1 outbred mice. *Reproductive Toxicology* 2008;26:231–8.
- [37] Salian S, Doshi T, Vanage G. Impairment in protein expression profile of testicular steroid receptor coregulators in male rat offspring perinatally exposed to bisphenol A. *Life Sciences* 2009;85:11–8.
- [38] Manikkam M, Guerrero-Bosagna C, Tracey R, Haque MM, Skinner MK. Transgenerational actions of environmental compounds on reproductive disease and epigenetic biomarkers of ancestral exposures. *PLoS ONE* 2012;7:e31901.
- [39] Bruner-Tran KL, Osteen KG. Developmental exposure to TCDD reduces fertility and negatively affects pregnancy outcomes across multiple generations. *Reproductive Toxicology* 2011;31:344–50.
- [40] Hoile SP, Lillycrop KA, Thomas NA, Hanson MA, Burdge GC. Dietary protein restriction during F0 pregnancy in rats induces transgenerational changes in the hepatic transcriptome in female offspring. *PLoS ONE* 2011;6:e21668.
- [41] Waterland RA, Travisano M, Tahiliani KG, Rached MT, Mirza S. Methyl donor supplementation prevents transgenerational amplification of obesity. *International Journal of Obesity* 2008;32:1373–9.
- [42] Painter RC, Osmond C, Gluckman P, Hanson M, Phillips DI, Roseboom TJ. Transgenerational effects of prenatal exposure to the Dutch famine on neonatal adiposity and health in later life. *BJOG* 2008;115:1243–9.
- [43] Greer EL, Maures TJ, Ucar D, Hauswirth AG, Mancini E, Lim JP, et al. Transgenerational epigenetic inheritance of longevity in *Caenorhabditis elegans*. *Nature* 2011;479:365–71.
- [44] Ruden DM, Lu X. Hsp90 affecting chromatin remodeling might explain transgenerational epigenetic inheritance in *Drosophila*. *Current Genomics* 2008;9:500–8.
- [45] Hauser MT, Aufsatz W, Jonak C, Luschnig C. Transgenerational epigenetic inheritance in plants. *Biochimica et Biophysica Acta* 2011;1809:459–68.
- [46] Rassoulzadegan M, Grandjean V, Gounon P, Vincent S, Gillot I, Cuzin F. RNA-mediated non-mendelian inheritance of an epigenetic change in the mouse. *Nature* 2006;441:469–74.
- [47] Wagner KD, Wagner N, Ghanbarian H, Grandjean V, Gounon P, Cuzin F, et al. RNA induction and inheritance of epigenetic cardiac hypertrophy in the mouse. *Developmental Cell* 2008;14:962–9.
- [48] Pembrey ME. Male-line transgenerational responses in humans. *Human Fertility (Cambridge, England)* 2010;13:268–71.
- [49] Koopman P, Munsterberg A, Capel B, Vivian N, Lovell-Badge R. Expression of a candidate sex-determining gene during mouse testis differentiation. *Nature* 1990;348:450–2.
- [50] Lees-Murdock DJ, Walsh CP. DNA methylation reprogramming in the germ line. *Epigenetics* 2008;3:5–13.
- [51] Kvist U, Bjorn Dahl L. Sperm motility. In: *Manual on Basic Semen Analysis*. ESHRE Monographs. Oxford, United Kingdom: Oxford University Press; 2002. p. 14–7.
- [52] Taylor GT, Weiss J, Frechmann T, Haller J. Copulation induces an acute increase in epididymal sperm numbers in rats. *Journal of Reproduction and Fertility* 1985;73:323–7.
- [53] Tateno H, Kimura Y, Yanagimachi R. Sonication per se is not as deleterious to sperm chromosomes as previously inferred. *Biology of Reproduction* 2000;63:341–6.
- [54] Atherton RW, Harris FL. A method for the fractionation and purification of sea urchin sperm development. *Growth & Differentiation* 1973;15:255–60.
- [55] Martinato F, Cesaroni M, Amati B, Guccione E. Analysis of Myc-induced histone modifications on target chromatin. *PLoS ONE* 2008;3:e3650.
- [56] Sadikovic B, Yoshimoto M, Al-Romaih K, Maire G, Zielenska M, Squire JA. In vitro analysis of integrated global high-resolution DNA methylation profiling with genomic imbalance and gene expression in osteosarcoma. *PLoS ONE* 2008;3:e2834.
- [57] Frith MC, Saunders NF, Kobe B, Bailey TL. Discovering sequence motifs with arbitrary insertions and deletions. *PLoS Computational Biology* 2008;4:e1000071.
- [58] Mahony S, Benos PV. STAMP: a web tool for exploring DNA-binding motif similarities. *Nucleic Acids Research* 2007;35:W253–8.
- [59] Inawaka K, Kawabe M, Takahashi S, Doi Y, Tomigahara Y, Tarui H, et al. Maternal exposure to anti-androgenic compounds, vinclozolin, flutamide and procymidone, has no effects on spermatogenesis and DNA methylation in male rats of subsequent generations. *Toxicology and Applied Pharmacology* 2009;237:178–87.
- [60] Schneider S, Kaufmann W, Buesen R, van Ravenzwaay B. Vinclozolin—the lack of a transgenerational effect after oral maternal exposure during organogenesis. *Reproductive Toxicology* 2008;25:352–60.
- [61] Nisenblat V, Norman RJ. Androgens and polycystic ovary syndrome. *Current Opinion in Endocrinology, Diabetes, and Obesity* 2009;16:224–31.
- [62] Menke MN, Strauss 3rd JF. Genetic approaches to polycystic ovarian syndrome. *Current Opinion in Obstetrics and Gynecology* 2007;19:355–9.
- [63] Long GG. Apparent mesonephric duct (rete anlage) origin for cysts and proliferative epithelial lesions in the mouse ovary. *Toxicologic Pathology* 2002;30:592–8.
- [64] Li Z, Huang H. Epigenetic abnormality: a possible mechanism underlying the fetal origin of polycystic ovary syndrome. *Medical Hypotheses* 2008;70:638–42.
- [65] Popp C, Dean W, Feng S, Cokus SJ, Andrews S, Pellegrini M, et al. Genome-wide erasure of DNA methylation in mouse primordial germ cells is affected by AID deficiency. *Nature* 2010;463:1101–5.
- [66] Li CC, Cropley JE, Cowley MJ, Preiss T, Martin DI, Suter CM. A sustained dietary change increases epigenetic variation in isogenic mice. *PLoS Genetics* 2011;7:e1001380.
- [67] Feinberg AP, Irizarry RA. Evolution in health and medicine Sackler colloquium: stochastic epigenetic variation as a driving force of development, evolutionary adaptation, and disease. *Proceedings of the National Academy of Sciences of the United States of America* 2010;107(Suppl. 1):1757–64.
- [68] Keverne B. Monoallelic gene expression and mammalian evolution. *Bioessays* 2009;31:1318–26.